Validating the openBCI Nodes through EEG-based BCI Application for Smart Home Automation Control

Adelina Kremenska, Anna Lekova, Svetoslav Kremenski, and Georgi Dimitrov

Original scientific article

***Abstract*—Advancements in portable EEG headsets have accelerated Brain-Computer Interface (BCI) applications, particularly in smart home automation and user well-being. However, few BCI platforms support cross-disciplinary users with limited programming skills. To address this, we propose a visual, node-based BCI programming framework using BrainFlow and the OpenBCI toolkit within Node-RED. This approach enables users to stream, process, and extract EEG features, while leveraging BrainFlow APIs as backend child processes to ensure adaptability and seamless updates. The framework was validated through a case study with 14 participants, where an OpenBCI headset was used to control a robotic arm. Results revealed that specific bursts in Event-Related Synchronization (ERS) within certain frequency bands were crucial for attention-based control. θ (theta) and γ (gamma) frequency bands in the frontal lobe were highly significant, as these regions are associated focus and decision-making. Similarly, high β (beta) activity in the left central and parietal lobes demonstrated a strong correlation with motor control and sustained attention. The study also evaluated the BrainFlow 'Mindfulness' metric to assess mental state during task engagement. The average value of this metric was 0.31, with a standard deviation of 0.11, indicating a moderate relative variability with a coefficient of variation ≈ 0.364. The results also highlight the key electrodes and frequency bands involved during attention and concentration, emphasizing the potential of using EEG-based metrics and ERS burst patterns as reliable neural markers to distinguish these states.**

***Index terms*—EEG-based Brain Computer Interface, Smart homes, IoT, OpenBCI, BrainFlow, Node-RED.**

I. Introduction

The expansion of Brain-Computer Interface (BCI) applications is strongly linked to the increasing accessibility of electroencephalography (EEG) hardware, particularly portable, noninvasive, wireless EEG headsets that often feature open-source software. Recent advances in BCI technology [1],[2] are driving the expansion of BCI applications, enabling seamless integration with smart home automation control systems [3-9] and enhancing user well-being [10],[2].

Back in 2003, Mason and Birch [11] defined the primary goal of BCI development as empowering individuals with disabilities to control electronic devices, thereby enhancing their communications and overall quality of life. These authors first proposed a functional model of a BCI system with its significant social impact. Then this topic is widely studied across multiple disciplines, and with Internet connectivity and IoT integration, the BCI system enables long-distance communication and control. However, only a few BCI frameworks and open-source platforms are specifically designed to assist cross-disciplinary professionals with limited programming skills in developing BCI applications with IoT integration, which is essential for smart home control [12-16]. The key advantage of toolkits [13] and [14] integrated in Node-RED [17] is their ability to streamline the connection to IoT devices and services. Node-RED is a visual programming tool with a web interface for designing applications by connecting prebuilt blocks, which represent various functionalities and processes. These blocks are arranged into flows, creating an intuitive graphical environment for designing BCI applications. Furthermore, [14] provides APIs to open-source software BrainFlow [18] for signal processing and EEG feature extraction regardless of the type of BCI boards. Calling the BrainFlow APIs from Python scripts as child processes in the backend, ensures adaptability to technological advancements and facilitates seamless updates. In contrast, the toolkits in [12], [15], and [16] do not utilize visual programming or prebuilt blocks and instead require programming expertise for integration with Python-based IoT frameworks, MQTT implementation, or calling external BCI APIs for smart home automation.

The main contribution of this research is a BCI framework to assist cross-disciplinary professionals with limited programming skills in developing BCI applications and integration based on prebuild nodes in open-source platform for visual programming. The methodology presented in [19] explains how to integrate portable EEG devices for smart home control via IoT using the OpenBCI toolkit in Node-RED. This work is further expanded here, including an extended overview of the functionality of nodes within the OpenBCI toolkit. Another extension involves validating the proposed framework with 7 additional participants in the same case study - a BCI application that uses BrainFlow performance metrics to control a TinkerKit Braccio robot arm [20] via OpenBCI Cyton + Daisy boards [21]. A detailed research protocol (provided as a supplementary file), along with materials and methods, supports the study. The new data were merged and analyzed to

Manuscript received February 5, 2025; revised March 19, 2025. Date of publication June 5, 2025. Date of current version June 5, 2025. The associate editor prof. Vladan Papić has been coordinating the review of this manuscript and approved it for publication.

This research was funded by the European Regional Development Fund under the Operational Program "Scientific Research, Innovation and Digitization for Smart Transformation 2021–2027", Project CoC "Smart Mechatronics, Eco- and Energy Saving Systems and Technologies", BG16RFPR002-1.014-0005 and National Scientific Research Fund, Project № KP-06-COST/14.

A. Kremenska, A. Lekova, and S. Kremenski are with the Institute of Robotics, Bulgarian Academy of Sciences, Bulgaria (e-mails: a.kostova012@gmail.com, a.lekova@ir.bas.bg, s_kremenski@yahoo.com).

G. Dimitrov is with the University of Library Studies and Information Technologies, Bulgaria (e-mail: g.dimitrov@unibit.bg).

Digital Object Identifier (DOI): 10.24138/jcomss-2025-0012

enhance the robustness of our findings. By re- analyzing the proposed in [19] mindfulness metric threshold and bursting in EEG activity, we reinforced our conclusions regarding the key electrodes and frequency bands involved during attention and concentration.

The paper is organized as follows: Section II presents related works. Section III describes the system architecture of an EEG-based BCI for communication with smart home automation control systems using openBCI toolkit in Node-RED library. Section IV describes the nodes in openBCI toolkit. Section V presents the research protocol, materials and methods. Results and discussion are in Section VI. Then conclusions follow.

II. Background and Related Works

Still in 2003, Mason and Birch [11] defined the primary goal of BCI development - to empower individuals with severe disabilities to control various electronic devices, greatly enhancing their communication abilities and overall quality of life. The expansion of BCI applications is driven by advancements in this technology [1], [2]. Noninvasive and portable EEG headsets, wireless EEG headsets that often feature open-source software, enabling seamless integration with smart home automation control systems and enhancing user well-being.

A. Related Works

Authors in [11] first proposed a functional model of a BCI system. Given its significant social impact, this topic is widely studied across multiple disciplines. With internet connectivity and IoT integration, the BCI system enables long-distance communication and control. BCI applications for smart home automation control systems have expanded [3÷9]. The state-of-the-art study in [3] explores BCI in medical applications, such as operating robotic arms, smart homes and smartphones, aiming to empower individuals with special needs to make autonomous decisions. It surveys how smart homes, equipped with smartphone-related technologies, enable inhabitants to control household devices like lights, fans, air conditioning and doors, as well as monitoring on smartphones. While these studies have explored BCI applications, most have used specific protocols and devices with small participant samples, limiting the generalizability of their findings. Additionally, most of BCI applications remain in the prototype stage. The BCI platform discussed in [4] integrates Artificial Intelligence of Things (AIoT) with cloud platforms to enhance the intelligence and functionality of smart homes, buildings and cities. It focuses on using sensors, lighting, meters and other connected devices to gather and analyze data, while addressing security and privacy concerns. In [5] supervised machine learning algorithms on EEG signals are used to train the classifier to recognize specific mental commands, which then are mapped to the corresponding actuator to alter its state. The digital twin is served as an intermediary to direct control commands from the brain signals to the actual asset. The authors in [6] explore the use of the Think Gear Application-Specific Integrated Circuit (TGAM) EEG Sensor Module, which enables single-channel analog EEG signal acquisition and is integrated with a Bluetooth module for wireless communication. This system supports IoT integration for long-distance communication and control, making it suitable for industrial automation and smart home device control, such as lights and doors, based on EEG signals. In [7] a system prototype is presented, consisting of the EMOTIV Insight headset, Raspberry Pi 4, a servo motor for opening and closing the door and LEDs, for disabled people. They can control the door and LEDs using their brain signals through a WebSocket connection to the Emotiv Cortex API. The system also includes a Flutter-based application to receive notifications on a smartphone for the status of the door and the LEDs. The BCI platform proposed in [8] integrates Node-RED for software communication between OpenVIBE outputs and the KNX protocol for the tasks' execution (regulation of two switching devices). The experimental results provide evidence of the effectiveness of the users' intentions classification, which has subsequently been used to operate the proposed home automation system, allowing users to operate two light bulbs. EEG data are recorded with the Emotiv EPOC X headset, and OpenVIBE was used for signal post-processing, feature extraction and classification. Then, Node-RED is employed to command hardware devices and provide feedback on device status. The BCI platform proposed in [9] also utilizes the Emotiv Insight headset, integrating Node-RED and Python for data processing and control. The platform provides new technical and practical directions for enabling remote experimentation using versatile software (Node-RED, MakeCode, Python, LabVIEW, EmotivPRO, EmotivBCI) and hardware (Emotiv Insight, Micro:Bit, Raspberry Pi).

Although, all cited BCI frameworks and platforms implement key functional components defined in [11]: User, Electrodes, Amplifiers, Feature Extractor, Feature Translator and Control Interface, two of them utilize prebuilt blocks and visual programming in Node-RED, whereas the others depend on specific protocols for BCI or smart home devices. In conclusion, there is a need for platforms to assist professionals with limited software skills in creating BCI applications for smart home control in the context of IoT. Such platforms are limited, and some of them are more user-friendly. These include the NeuroScale [12], which integrates with widely used EEG devices in research and clinical settings, the EmotivBCI Node-RED toolkit [13], the openBCI Node-RED toolkit [14], MetaBCI [15] and OpenViBE [16]. The advantage of using [13] and [14] Node-RED, compared to the NeuroScale, MetaBCI, and OpenViBE approaches, lies in streamlining the integration process through visual programming and predefined blocks. For instance, when interfacing EEG headsets with a robotic arm, the prebuilt blocks of EmotivBCI Node-RED toolkit should connect the prebuild blocks for the robotic arm via COM port within a flow in Node-RED [17]. In contrast, the approaches in [12], [15] and [16] require programming skills for integration with Python-based IoT frameworks, implementing MQTT, or external APIs for smart home automation.

In summary, there is a need for a general framework to create BCI applications that can record, process and connect with various IoT devices and services, specifically designed to support professionals with limited software skills in developing BCI applications for smart home control. Given that Emotiv EEG hardware and OpenBCI hardware are among the most commonly used, we believe a BCI framework utilizing Node-RED and BrainFlow is the optimal technical solution, as a

toolkit specifically tailored to OpenBCI headsets. Additionally, [22] lists 230 research papers utilizing OpenBCI hardware, with publications spanning from 2023 to 2025 (accessed in January 2025), and cites [19] as well.

B. Node-RED and BrainFlow Software Library

Both Node-RED and BrainFlow are open-source, providing easy access for developing BCI applications. Node-RED is a visual programming tool with a web interface that allows users to design applications by connecting prebuilt blocks, or 'nodes', which represent various functionalities and processes. These blocks are organized into flows, providing a highly intuitive environment for building BCI applications without needing to write text code. Node-RED supports integration with a wide variety of devices, APIs and services, making it particularly useful for IoT applications, home automation and real-time data monitoring. While the EmotivBCI Toolkit is specific only to three Emotiv devices, the openBCI nodes supports more than 20 open-source EEG boards through the BrainFlow software library [23] and provide uniform data acquisition API for these boards. The openBCI toolkit uses the BrainFlow library that helps in signal acquisition and processing, managing Python scripts for board interaction, real-time EEG data streaming, data sampling, sliding window techniques, power spectral density decomposition, etc. Additionally, calling BrainFlow APIs from Python scripts as child processes in the backend ensures adaptability to technological advancements and facilitates seamless updates.

In conclusion, node-based visual programming streamlines the integration of BCI with smart home automation applications. In this context, we propose a framework specifically designed to assist cross-disciplinary professionals with limited programming skills in developing BCI applications with IoT integration through visual node-based programming, built using the BrainFlow library within the Node-RED platform. Additionally, Section III presents a system architecture that explains how the openBCI toolkit can be utilized within Node-RED.

III. System Architecture

The system architecture for an EEG-based BCI has been designed and developed to facilitate communication with IoT devices and services using the openBCI toolkit in Node-RED, with application capabilities for smart home automation control (Fig.1). To register EEG signals, a non-invasive and portable EEG device, OpenBCI, was utilized. However, within the established architecture, other EEG devices supported by the BrainFlow library can also be employed. The measured EEG data is transmitted via Bluetooth to the Node-RED, and the system also supports data transmission over Wi-Fi. Node-RED serves as a browser-based tool for streamlining programming flows and acts as a gateway to the IoT, enabling the sending of JSON-type requests to the FlowFuse platform, used for cloud computing within the Sensetecnic cloud. This setup allows the BCI device to connect to cloud-based computational services and execute actions with smart home automation control devices or services.

The architecture provides users with the flexibility to use various EEG devices. To support this, three new nodes were added to the Node-RED library (Fig.2): 'openBCI-streaming,' 'openBCI-Data,' and 'openBCI-EEGmetrics.' These customized nodes provide access to the BrainFlow API, tailored to the selected device and processing requirements. BrainFlow is a software framework designed for building BCI applications with conventional programming languages, supporting over twenty EEG-based BCI devices.

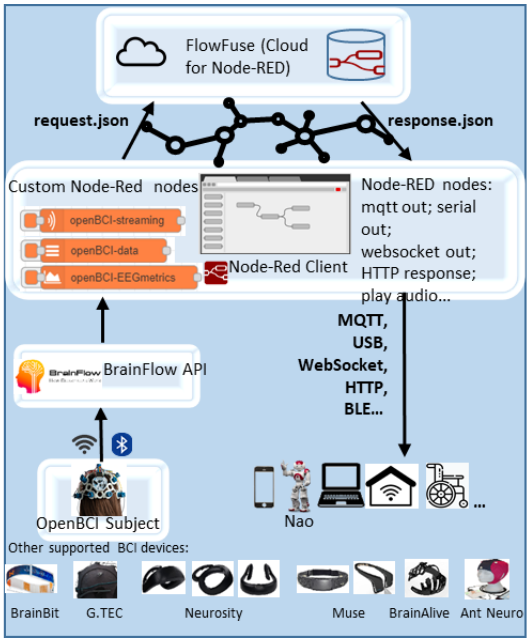

Fig. 1. A system architecture for an EEG-based BCI in the IoT, utilizing the openBCI toolkit within Node-RED.

These nodes enable users to transform BCI devices into “things” through Node-RED, removing the need for any programming code. This approach expands the capabilities of Node-RED, allowing OpenBCI users to easily specify the board ID, data type, and electrodes of interest. Based on user input in the node settings, a JavaScript file within the node processes and passes the parameters to the BrainFlow API. This transmission occurs through a child process linking the Node.js server in Node-RED to the BrainFlow API, where the output is generated in JSON type. The connection between Node.js and the BrainFlow API is facilitated by a newly developed Python file utilizing BrainFlow libraries. Each newly created node contains this file in its directory, which varies depending on the specific functionality of the node. Node-RED also provides various output nodes, such as mqtt out, serial out, http response, play audio, and generic-BLE out, for subsequent data transmission to IoT devices and services.

IV. New Nodes in openBCI Toolkit for Node-RED

In our previous work [19], we introduced an initial set of OpenBCI nodes for Node-RED, enabling seamless integration of EEG-based BCI with smart home automation systems. These nodes provided the necessary functionalities for EEG signal acquisition, streaming, preprocessing and featuring with the event-based control mechanisms. While the core functionality of these nodes is unchanged, this extended work offers clearer,

more structured descriptions of their capabilities. It includes improved explanations, configuration options, and real-world use case, along with refined implementation guidelines for smart home automation.

In this section, we provide a detailed summary of the user settings and functionalities of each new node available in the Node-RED palette (Fig. 2). The goal is to offer clear guidance to users on how to configure and utilize these nodes effectively within their design process. Each node's parameters, input-output behavior, and customization options are outlined to help users understand its role within a BCI system. By detailing these settings, we aim to simplify the integration of openBCI nodes into Node-RED workflows, ensuring that users can optimize their configurations for real-time signal processing, event detection, and smart home automation control.

Fig. 2. Visualization of the openBCI nodes in the Node-RED palette

A comprehensive flowchart illustrating the developed original methods and algorithms for visual programming and the integration of a BCI into a web-based streaming environment is presented in detail in [24]. The flowchart illustrates the working principle of the developed original methods and algorithms used in the overall operational process of each new node. These nodes integrate various software technologies and programming languages, including HTML, JavaScript, Python, Express, and others, with the flowchart highlighting the logical connections between them. While the diagram is specifically designed for the "openBCI-data" node, the underlying principles are also applicable to the other two newly created nodes—"openBCI-streaming" and "openBCI-EEGmetrics."

The front-end of each node is responsible for visualizing the node's output and is built using HTML and JavaScript. This section of the node interacts with the visual elements displayed in the web interface, structured in an .html file within the node's directory. The back-end of each node is implemented entirely in JavaScript, encapsulated in two .js files located within the node's directory. These files define the server-side logic, data handling, and communication with other components of the system. A connection from the Node-RED Node.js server to the Brainflow API was established through the use of a second .js file, which utilizes the child_process module to execute a newly developed Python file. The Node.js child_process module allows access to operating system functionalities by executing system commands in a child process. This module provides control over the arguments passed to the OS command and enables the use of the command's output, which in this case facilitates the integration of the Brainflow API for EEG signal acquisition and processing. The EEG data collection and processing section of the new nodes is managed through Python, specifically in a .py file within the node's directory. The flowchart illustrates how data flows from the front-end through the back-end, where it is processed by the Python code to handle EEG data effectively. Finally, the concluding processes of each node, such as data analysis and transmission to other systems, are visualized in the flowchart, completing the entire data handling and processing cycle.

In the initial stages of development, a limitation was observed with EEG devices transmitting data via USB dongle through the COM port, restricting the initiation of only one process per port. This limitation prevents the simultaneous collection and processing of data from different sources and/or electrodes, necessitating that all conditions be handled within a single process and session. To overcome this, we utilized the BrainFlow streaming board to stream data to various destinations such as files or sockets directly from BrainFlow. With this method, subsequent data collection and processing processes are initiated not with the main board but with the BrainFlow streaming board, allowing the user to configure multiple micro-processes through visual programming while maintaining only one main process to the COM port.

These three nodes have been developed with a set of custom user settings that provide users with various configuration options. When used correctly, they enable multiple use cases for researchers and IoT enthusiasts, catering to different needs and scenarios. To ensure proper usage, a detailed user guide is provided during the installation process, which explains the setup and functionality of each node. Figure 3 illustrates an overview of the settings for the "openBCI-data" node, which is the most complex of the three and offers the widest range of configuration options. These settings allow users to define parameters such as board IDs, data types, and specific electrodes of interest. The flexibility provided by these options ensures that the nodes can be adapted to a wide range of applications, from simple data streaming to more advanced EEG metric analyses. By tailoring the settings to specific requirements, users can maximize the potential of their BCI system within the IoT ecosystem.

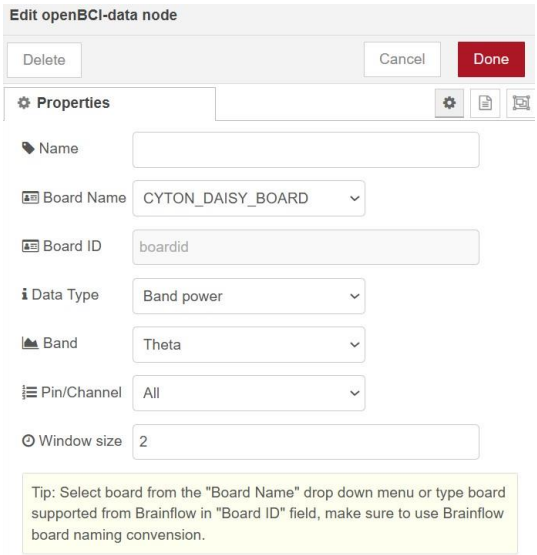

Fig. 3. Overview of the User settings of the ‘openBCI-data’ node within Node-RED

C. Node 'openBCI-streaming'

The 'openBCI-streaming' node serves a critical role in establishing and managing the streaming session between Node-RED and the OpenBCI EEG device via the BrainFlow API. It launches the primary process to the OpenBCI board and initiates the data stream, enabling the real-time collection of EEG data. This data can then be processed and utilized in various applications, such as smart home automation control and BCI systems. This node essentially acts as the gateway for live EEG data, allowing for seamless communication between Node-RED workflows and the OpenBCI hardware. The front-end of the 'openBCI-streaming' node provides a 'Board Name' dropdown menu, allowing users to select from a list of OpenBCI boards available via the BrainFlow API. This selection automatically disables the 'Board ID' field to prevent user error, ensuring that the correct device is chosen. Alternatively, users can manually input the 'Board ID' if they prefer, offering flexibility for specific configurations. Additionally, the 'Serial Port' field is used to specify the COM port to which the OpenBCI board is connected, ensuring the correct connection to the EEG hardware. Users also configure the 'Streaming Time (Seconds)' field, which defines the duration for which the EEG data will be streamed. Once the session duration is reached, the node sends a 'Stop stream' JSON message to signal the end of the session, ensuring smooth termination. The node is positioned within the newly created openBCI category in the Node-RED palette after installation. It is configured with a button for immediate start and an input for initiation via another Node-RED node, providing flexibility in how the streaming session is triggered. To begin a session, users must know the exact COM port used by their EEG device for proper registration. Upon node initiation, the algorithm establishes a session with the 'streaming' BrainFlow board and outputs a 'Start stream' debug message, confirming that the data collection process has started. When the node is triggered, either via the button in the Node-RED interface or through another node in the flow, it begins streaming EEG data in real time. Once the user-defined streaming duration elapses, the node automatically sends a 'Stop stream' JSON message, signaling the conclusion of the session. A summary of the node is presented in Table I.

TABLE I
SUMMARY OF 'OPENBCI-STREAMING' NODE

Function	Initiates the main process to the OpenBCI board in Node-RED.
Configuration	Can be started with a button or another Node-RED node. (Applies for each new node)
User Settings	Requires 'Board Name' or 'Board ID,' 'Serial port,' and 'Streaming time (in seconds)'. The node automates the use of either 'Board Name' or 'Board ID' to avoid user errors.
Operation	Starts a streaming session, sends a 'Start stream' debug message, and after the specified streaming time, sends a 'Stop stream' JSON message.

D. Node 'openBCI-data'

The 'openBCI-data' node serves an essential function in processing EEG data in real time, providing users with three key functionalities: retrieving raw EEG signals, applying predefined signal filters, and calculating the power of specific EEG frequency bands. By enabling data processing within a Node-RED workflow, it allows researchers and developers to extract meaningful insights from EEG signals without requiring extensive programming knowledge. Unlike the 'openBCI-streaming' node, which is responsible for acquiring EEG data from the OpenBCI board, the 'openBCI-data' node focuses on analyzing and refining this data. However, it is not a standalone node—it depends on a functioning 'openBCI-streaming' node to supply continuous EEG input. Without an active streaming session, the 'openBCI-data' node cannot execute its processing algorithms. To ensure compatibility and flexibility, the 'openBCI-data' node offers several user-configurable settings. One of the primary requirements is selecting the 'Board Name' or entering the 'Board ID' to identify the EEG device. This selection must remain consistent across all nodes within the Node-RED workflow to maintain data integrity and avoid communication errors. The node consists also a 'Data Type' dropdown menu, which provides three options: RAW, Band Power, and Signal Filtering. The default selection is RAW, which allows users to access unprocessed EEG data directly from the OpenBCI board. The 'Window Size' field determines the duration of data visualization, expressed in seconds, giving users control over the time frame of displayed signals. If the 'Band Power' option is selected, an additional 'Band' field appears, allowing users to choose from seven EEG frequency bands: Delta'(δ), 'Alpha' (α), 'Theta' (θ), 'LowBeta'(β1), 'HighBeta' (β2), 'Gamma'(γ) or 'All'. This setting enables real-time computation of the power of the selected frequency band for a specific EEG channel, with results output in JSON format. For users interested in signal preprocessing, the 'Signal Filtering' option provides a supplementary menu where different filter types can be selected, including "Bandpass", "Bandstop", "Lowpass", "Highpass", "Rolling filter" and "Remove environmental noise". When activated, the node applies the chosen filter to the raw EEG data and outputs the processed signal in JSON format. The 'openBCI-data' node enhances EEG processing for research, assistive technology, and smart home automation, where EEG signals can trigger actions like adjusting lighting, controlling appliances, or customizing environmental settings based on cognitive states. Table II provides the summary of the node.

TABLE II
SUMMARY OF 'OPENBCI-DATA' NODE

Function	Retrieve raw data from the EEG device, or apply predefined filters to EEG data, or compute the powers of six frequency bands.
Dependencies	Requires a correctly functioning 'openBCI-streaming' node.
User Settings	Requires 'Board Name' or 'Board ID'. Provides options for 'Data type' (RAW, Band power, Signal filtering).
Operation	A. RAW: Accesses raw data with a specified time window. B. Band power: Calculates the power of a selected frequency band (e.g., 'Alpha', 'Theta'). C. Signal filtering: Filters raw data based on selected filter type (e.g., Bandpass, Lowpass).

D. Node 'openBCI-EEGmetrics'

The "openBCI-EEGmetrics" node, outlined in Table III, was developed to evaluate the focus and relaxation levels of the

individual wearing the EEG device. Its primary function is to calculate real-time metrics for both "Relaxation" and "Concentration" by analyzing brain wave activity. Developer can select either "Relaxation" or "Concentration" from the "Metric type" dropdown menu, which then triggers the algorithm to compute the corresponding metric using data from the EEG signals. The Brainflow API powers this computation, with the results returned as values between 0 and 1. When "Relaxation" is selected, the algorithm focuses on brain wave activity associated with closed-eye meditation, analyzing frequencies in the delta, theta, and alpha bands. Conversely, when "Concentration" is chosen, the algorithm examines beta and gamma brain waves, typically associated with maintaining focused attention while the eyes are open. This makes the "openBCI-EEGmetrics" node particularly valuable for applications in cognitive research, neurofeedback, and BCI-based control systems. The node operates using the Regression classifier by default, although the Brainflow API also provides options for other classifiers, including LDA, KNN, and SVM, offering flexibility for more advanced users. Additionally, the node calculates metrics across all channels in use, and users can adjust the "Window size" field to specify the time window (in seconds) for averaging the power of the selected frequency band, providing fine-tuned control over the data analysis process. In practical applications, the "openBCI-EEGmetrics" node can be used for monitoring mental states in real-time. For example, it could be applied in neurofeedback sessions to train users to achieve specific focus or relaxation states. It also has potential uses in smart home automation, where the subject's level of concentration or relaxation could trigger actions, such as adjusting the environment (e.g., lighting, sound) based on the user's cognitive state.

TABLE III
SUMMARY OF 'OPENBCI-EEGMETRICS ' NODE

Function	Monitors levels of focus and meditation.
User Settings	Allows selection of "Metric type" (Relaxation or Concentration). The user can set the time window for calculating the average power of the frequency band in the "Window size" field.
Operation	Uses the BrainFlow API to calculate metrics based on specific brain waves. The metrics are returned as values between 0 and 1, using Regression as the classifier by default.

V. MATERIALS AND METHODS

The proposed visual node-based programming framework for BCI applications was implemented and validated using an OpenBCI headset. In the described case study, the integration involved connecting the openBCI Node-RED toolbox with an Arduino-based robotic arm, allowing it to be controlled by concentration and attention. Simultaneously, the registered and processed EEG data were transmitted to a fuzzy inference service, specifically designed and implemented to validate the related published neuroscience findings and facilitate gathering knowledge from experiments.

A. Hardware

In this scientific experiment, the EEG-based OpenBCI Cyton + Daisy Boards (16-Channels with resolution 250 Hz) are used to control a TinkerKit Braccio robot arm within a Node-RED environment, simulating neural control of "things" in smart homes. For registering and processing the EEG data, a Dell laptop with an 11th Gen Intel(R) Core(TM) i7-1165G7 @ 2.80GHz processor was used. An Android-based tablet was utilized to present math problems involving addition and division of floating-point numbers that require memorizing intermediate calculations, with feedback for correct or wrong answer.

B. Scientific Context

The performance metric in Brainflow library to evaluate Mindfulness (focusing one's concentration) is based on various algorithms and techniques from the field of neuroscience and signal processing. The supported Concentration and Relaxation calculation from EEG data are based on Logistic Regression Classifier. Implementation details how to calculate derivative metrics from raw data can be seen in BrainFlow User API [23].

We integrated the expertise from the published neuroscientific research that correlates with concentration in a linguistic IF-THEN fuzzy rules, where fuzzy sets participate in the antecedence part for consecutive fuzzy inference.

Many studies have separately identified increased in several brain wave frequency bands in different locations during cognitive processes, that require concentration and memory functions. Both θ and β_2 waves are involved in active thinking and problem solving, whereas γ waves facilitate high-level cognitive functions and the integration of information [25]. Higher θ power is associated with cognitive engagement and memory processes and is critical for memory encoding and retrieval [25], [26] and [27]. Increasing of β_2 power is linked to active concentration and problem-solving, whereas γ power increased at some locations [26]. These brain waves work together to support various aspects of cognitive processing and memory functions, each contributing uniquely to the overall activity of the brain. For instance, high-frequency subcycles (40 Hz) occur within the broader framework of low-frequency oscillations (5 to 12 Hz) during short-term memory processes [26]. The most reported brain locations are prefrontal, frontal, central and Hippocampus [28]. Furthermore, θ/β ratio and θ/γ ratio have been widely studied as a marker of cognitive processing capacity [29], [30] and [26]. In [29] θ/β ratio is measured at Fz, Cz and Pz, while in [30] EEG spectral analysis found the role of electrodes Cz, P3, P4, Pz during attention. Jung et al in [31] found that the ratio of θ to α power as an indicator of alertness in different tasks. The study included frontal (F3, Fz, F4), central (C3, Cz, C4), and parietal (P3, Pz, P4) electrodes. In [32] authors also identified some of the mentioned features and electrodes that are indicative of attentiveness. Both θ/γ ratio and α/θ ratio are discussed in [26] and [27].

Based on these neuroscience findings, we expected to observe that the ongoing ERS in the frequency bands showed specific evoked bursts (ERS") in θ correlated with memory processes, β_2 correlated to active cognitive processing and attention, and γ correlated to concentration, over the prefrontal, parietal and motor cortexes. The electrodes of interests are: Frontal region electrodes: AF3, AF4, F3, F4, F7, F8; Central region electrodes: FC5, FC6, Cz and Parietal region electrodes: P3, P4, Pz.

C. Participants

In our previous work [19], we reported results from a study involving 7 participants. To improve the robustness of our findings, we conducted additional experiments with eight more participants, one female (43 years) and seven males (average age- 21 years). One participant, the female, was excluded from the analysis due to poor EEG signal quality. The data from the new participants were averaged together with the original dataset, resulting in a combined sample of 14 healthy participants (4 females and 10 males) with an average age of 26.28 years, all with technical background. Although the results in the current study can't be generalized, future work will include of more diverse participants and more diverse fields of education to obtain broader neuro insights about concentration. Each experimental session lasted about 30 minutes. All participants were acquired in details with the research protocol and with the safety and regulatory compliances of OpenBCI Cyton+Daisy boards for EU. Informed consent from all participants were obtained.

D. Experimental Task and Trial Setup

Participants were seated comfortably in front of TinkerKit Braccio robot arm (Fig.4) and the experiment task responses in activating the robot arm gripper.

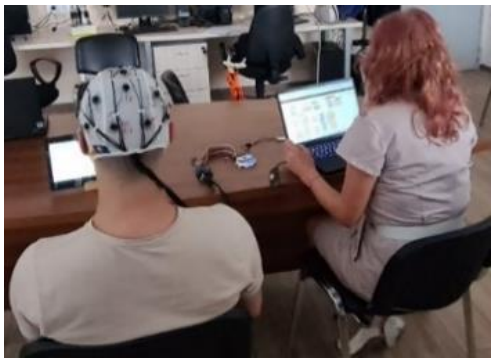

Fig. 4. Participant seated in front of TinkerKit Braccio robot arm

The participants performed math task two times (two sessions). We stimulate the participant's concentration and attention by simple math equations on a white screen. We distinguish attention and concentration according to the openbci-EEGmetrics Mindfulness Value (MV). At the beginning of the experiment a baseline phase for the MV, frequency bands and electrodes of interest were performed. In a rest state three fuzzy sets for Mindfulness (reference, low and high) were determined and used as reference, as well for the ERS″ for the average power of θ, α, β_2 and γ bands oscillation. Thus, the baseline for each participant were setup. The experiment started with an auditory cue (beep sound) and only when the robot arm had been activated (MV membership to fuzzy set high) the MV and ERS″ were recorded in csv files for post-hoc analysis. Figure 5 illustrates the block-based methodology used to structure the trial task, highlighting the key procedural steps. Each step is represented by a labeled block, with arrows indicating the sequence of operations.

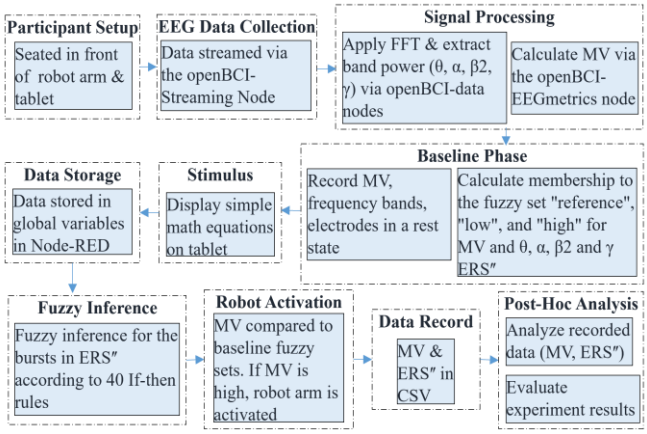

Fig. 5. Block-based methodology for the trial task

E. EEG Data Acquisition

The EEG data was continuously registered and wirelessly transmitted via the neuroheadset. A web session was established with a streaming server through a flow with 'openBCI-streaming' node, and the data was stored in global variables within Node-RED by that flow. The raw EEG signals from the electrodes were pre-processed using FFT to analyze frequencies ranging from 4 to 45 Hz. These frequencies were categorized into four main types: θ, α, β_2 and γ. The FFT output was then converted to power density ($\mu V^2/Hz$). This signal processing was implemented in a Node-RED flow developed with a set of data nodes configured using specific user-defined settings (Fig. 3). These nodes were programmed with the board ID for the Cyton + Daisy board and the data type set to "band power." Each node was assigned a specific band power of interest (e.g. δ, θ, α, β_1, β_2 or γ) and a corresponding channel of interest. The channels (1 to 12) represent the physical connections of the wires to the electrodes on the EEG cap, following the internationally recognized 10-20 system. This system ensures standardized electrode placement for consistent and reliable data collection. By configuring the nodes in this way, researchers could focus on the desired frequency bands and brain regions relevant to the experiment, facilitating targeted data analysis and application.

F. Methods

Four flows in Node-RED have been designed and developed to control the experiment. The first one exploits the presented in Section III, openBCI toolbox for Node-RED. The remaining flows are based on the fuzzy shell proposed in [33] for developing a custom EEG-based BCI, with the fourth flow mapping EEG activity to Arduino-based commands for a robot arm. The "csv node" from the Node-RED library was used to handle data formatted as comma-separated values and to record bursts in ERS of band power for post-hoc analysis.

F.1. Flow Design using openBCI Toolbox

The integration of data streams from the OpenBCI headset to Node-RED is facilitated through custom input nodes in 'openBCI' category, with installation details, node descriptions and usage provided in [24].

The used EEG markers and electrodes are AF3 (β_2, θ, γ), AF4 (β_2, θ, γ), F3 (θ, γ), F4 (θ, γ), F7 (α, θ), F8 (α, θ), FC5 (θ, γ), FC6 (θ, γ), Cz (θ, β_2), Pz (θ, β_2), P3 (θ, β_2), P4 (θ, β_2).

F.2 TinkerKit Braccio Robot Arm Control

The brainwave data collected by the boards is processed and classified in real time. When the Mindfulness Value (MV) is identified within the "high" fuzzy set, it triggers a lifting movement of the TinkerKit Braccio robotic arm, causing it to lift and then return to its resting position. The lift command is sent from a 'serial out' node in Node-RED to the arm. Upon receipt of this command, custom Arduino code, written and uploaded via the Arduino IDE, controls the arm's movements. The signal-to-action mapping is direct: the EEG-detected state activates the start command, which in turn initiates a predefined sequence of movements encoded in the Arduino. The arm's movement was triggered to visually indicate to participants that they were in a state of focused awareness.

F.3 Connectivity to Local Fuzzy Inference Service

The designed and implemented fuzzy model uses trapezoidal membership functions and Takagi-Sugeno-Kang (TSK) fuzzy inference. The conceptual model how to evaluate the bursts in the frequency powers by TSK fuzzy logic is presented in Fig.6, showing how the model is integrated with EEG data and how the fuzzy membership sets are initialized.

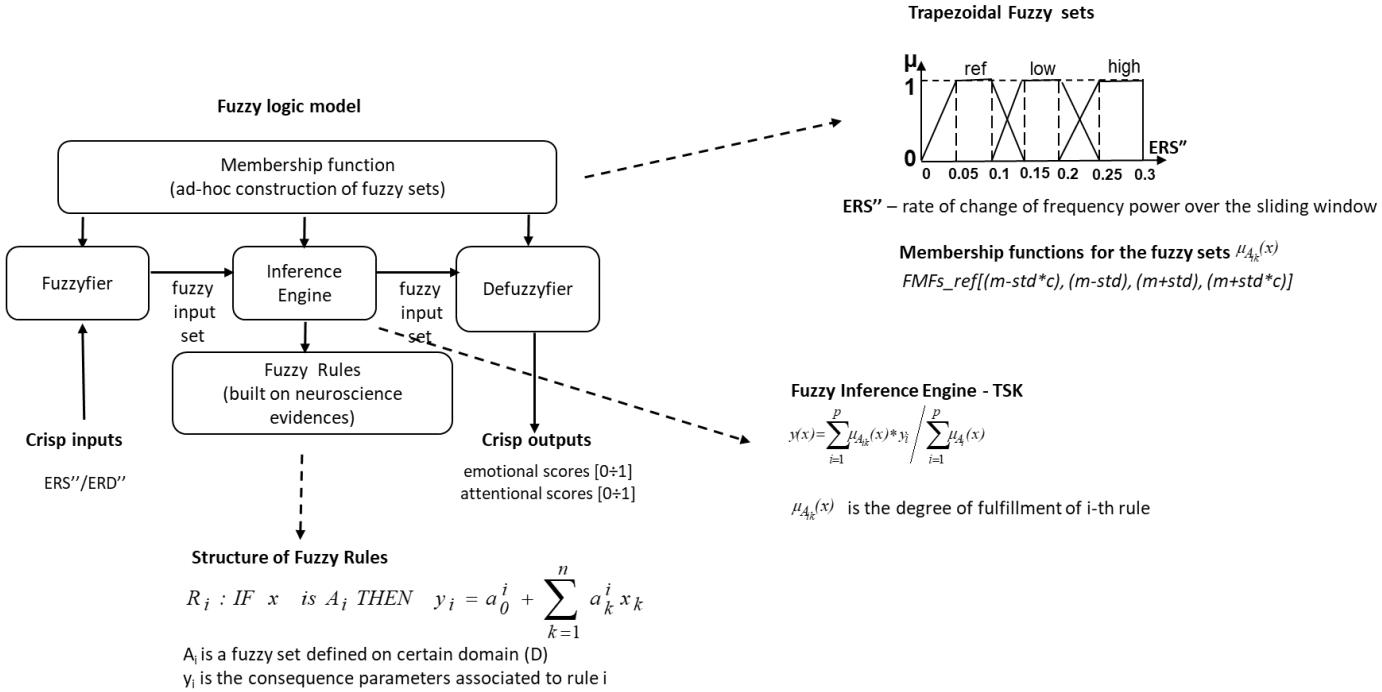

Fig. 6. Takagi-Sugeno-Kang (TSK) fuzzy model for evaluating the rate of change of frequency powers

Figure 7 presents a more detailed description of the model, illustrating how the fuzzy inference is performed. Based on this model, two flows use the OpenBCI data: one for baseline and one for data analysis with uncertainties. In Node-RED, these flows perform the reference phase and generate the fuzzy sets and fuzzy membership functions. The membership functions for the fuzzy sets (FMFs) were built during the baseline phase:

$$\text{FMFs\_ref}[(\text{m} - \text{std} * \text{c}), (\text{m} - \text{std}), (\text{m} + \text{std}), (\text{m} + \text{std} * \text{c})] \quad (1)$$

where *c* is a tuning parameter, *m* is the mean and *std* is the standard deviation obtained from 150 samples during the baseline. The value of *c* parameter can be obtained based on experience or by an optimization procedure as presented in [33].

The flow in Node-RED that implements the fuzzy inference service can be seen in Figure 8. The published neuro expertise that correlates with the EEG activities of participants related to attention and concentration was translated into 14 interpretable fuzzy IF-THEN rules for θ/β ratio and θ/γ ratio. Additionally, 26 fuzzy IF-THEN rules were developed to distinguish the most important EEG markers and electrodes mentioned in Subsection *F1*. We evaluated the second derivative of ERS (featured by ERS″) and applied fuzzy rules and Sugeno-style aggregation of the rule outputs. The role of second derivative of ERS in EEG frequency powers is relative and slightly influenced by baseline calibration, used to distinguish normal fluctuations from significant events. While baseline shifts (due to a poor contact with the scalp, muscle activity or eye movements) can slightly affect detection sensitivity, EEG bursts like beta or gamma events still maintain identifiable temporal and spectral signatures.

Even in the presence of artifacts, these bursts remain detectable. The role of the TSK fuzzy system is the computational efficiency, because unlike Mamdani inference, TSK inference avoids complex defuzzification, making it faster and more practical for real-time applications. Another advantage is that only critical changes are described in fuzzy rules *(FR)* at source and scalp level, or when testing a condition with contradictions in assumptions.

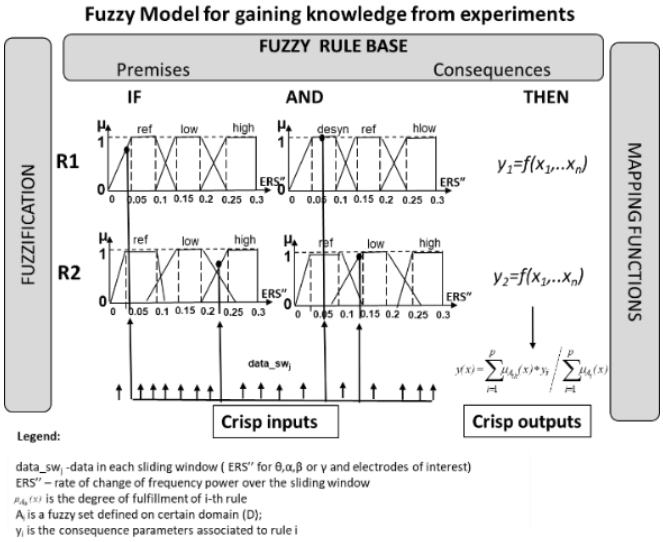

Fig. 7. Detailed description of the model how the fuzzy inference is performed

The bursts in θ, α, β2 and γ are featured by ERS″ and labeled for each trial and epoch based on the status of the fuzzy sets for mindfulness (high and low). Each training sample is associated with a label *(l)* corresponding to the current condition *(C)* of a single class, (l_{i_C}). The first label (l_{1_C}) corresponds to the *low* MV condition, the second label (l_{2_C}) corresponds to the *high* MV condition, and the third label (l_{3_C}) - to theta/gamma synchrony. ERS″ bursts over the scalp site and bandwidth were evaluated in windows with a length of 250 msec. and a step size of 125 msec. Instances of how the bursts in θ, α, β2 and γ for the electrodes of interest reflect the functional connectivity for the fronto-central alpha/theta power asymmetry are expressed as follows in FR7 and FR8:

$$\text{IF "F7\_T\_ERS", "high" } AND \text{ "F7\_A\_ERS", "ref", } THEN\ l_{2_C}$$
$$\text{IF "F8\_T\_ERS", "high", "F8\_A\_ERS", "ref", } THEN\ l_{2_C}$$

where *F7 T ERS* is a linguistics variable with fuzzy set "high". Other options are "low" and "ref". *F7_T_ERS″* means that a positive-going θ power over a right-frontal electrode site displays maximum rate for the power increase with a peak latency of 250 *msec*, mapping brain activity, while there is negative-going α power for *F7_A_ERS″* in this epoch. FR9 expresses the functional connectivity for the theta/gamma synchrony for electrode F3:

$$\text{IF "F3\_G\_ERS", "high", "F3\_T\_ERS"250", "ref", } THEN\ l_{3_C}$$

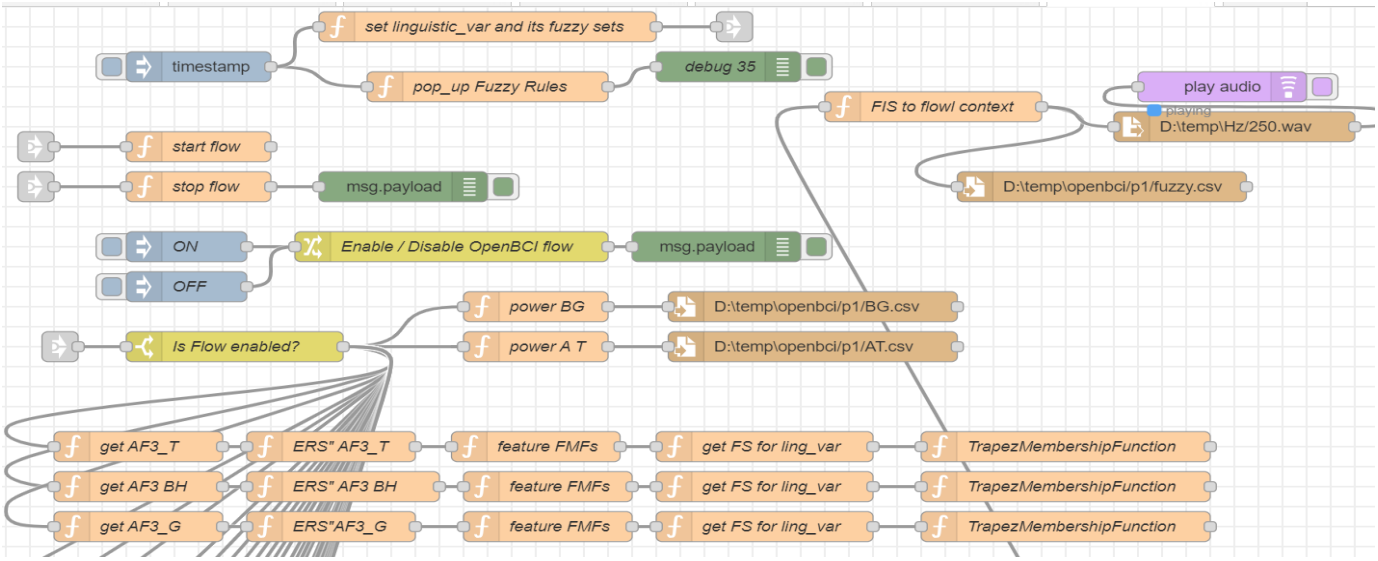

Fig. 8. Node-RED flow that implements the fuzzy inference service

F.4 OpenBCI-EEGmetrics MINDFULNESS (Attention and Concentration) value

Since participants exhibit different values within the interval [0,1] for mindfulness, we define fuzzy membership functions (FMFs) for three fuzzy sets ["reference", "low", and "high"] during the baseline phase to differentiate their states during rest versus concentration. The fuzzy set "high" is a right-angled trapezoid (see Fig.6). The participants' FMFs were calculated based on the mean and standard deviation of the measured MV in the resting state. The formula used to calculate the FMFs is given by Equation (1).

During math problem-solving, if the mindfulness value falls within the "low" or "high" fuzzy set, we detect attention and concentration at different levels of intensity. The "low" fuzzy set is also considered to ensure that no bursts are missed in that case.

G. EEG Data Analysis

Concentration-related bursts in time for the electrodes in four frequencies were analyzed. The evoked ERS″ were averaged across all participants. We concatenated all experiments into one big matrix to produce a grand average in order to discriminate the burst at site level and frequencies. The post-hoc interpretation of the results by ANOVA revealed that the mean values for ERS″ in the fuzzy rules fired during

mindfulness in the fuzzy set 'high' are most significant for the electrodes and band powers shown in Figure 9. The F-statistic value (14.64) is high, indicating strong differences between the groups being compared (see Table IV), and with $p < 0.001$, the test provides strong evidence of statistical significance.

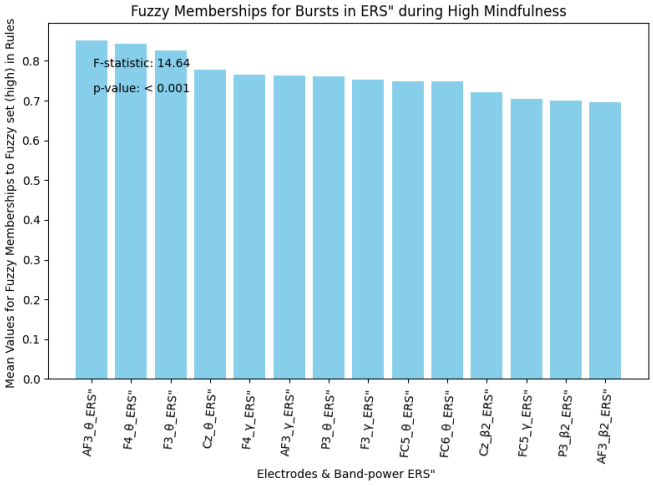

Fig. 9. Mean values of fuzzy membership grades for bursts in ERS during mindfulness in the "high" fuzzy set

TABLE IV
STATISTICALLY SIGNIFICANT RESULTS ($P < 0.05$) FROM THE PAIRED-SAMPLE T-TEST FOR ERS" FOR EACH RULE

ERS" vs ERS"	AF3_γ	AF3_θ	Cz_β2	Cz_θ	F3_γ	F3_θ	F4_γ	F4_θ	FC5_γ	FC5_θ	FC6_θ	P3_β2	P3_θ
AF3_β2	0.1293	0.2172	0.0934	0.2411	0.1243	0.1906	0.1362	0.2066	0.085	0.1234	0.1208	0.0761	0.4163
AF3_γ		0.147	p<0.05	0.1733	0.0545	0.1203	0.0664	0.1363	p<0.05	0.0537	0.051	p<0.05	0.3493
AF3_θ			0.0674	0.0833	p<0.05	p<0.05	p<0.05	p<0.05	0.0751	p<0.05	p<0.05	0.0844	0.2596
Cz_β2				0.2159	0.0997	0.1662	0.1117	0.1821	0.0603	0.0988	0.0962	0.0514	0.3908
Cz_θ					0.1353	0.2063	0.1473	0.2225	0.0912	0.1332	0.1314	0.0849	0.364
F3_γ						0.1371	0.0825	0.1531	p<0.05	0.0696	0.067	p<0.05	0.361
F3_θ							p<0.05	0.0699	p<0.05	p<0.05	p<0.05	0.0594	0.2852
F4_γ								0.1406	p<0.05	0.0572	0.0546	p<0.05	0.3487
F4_θ									0.0668	p<0.05	p<0.05	0.0761	0.2688
FC5_γ										0.1256	0.1232	p<0.05	0.4106
FC5_θ											0.0718	p<0.05	0.3643
FC6_θ												p<0.05	0.3653
P3_β2													0.4138

The significant values are observed mainly in the left side, and particularly θ and γ activity in the frontal lobe, β_2 - in left central and parietal lobes. For α ERS we don't observe significant bursts.

The experimental conclusions derived from the interpretation of the ERS″ means over time reveal also θ/γ synchrony in samples with a resolution of 250 Hz. Figure 10 illustrates the bursting and the instantaneous coupling of θ and γ frequencies for the F3 electrode. We interpreted this nested structure as enabling the brain to efficiently organize and separate various pieces of information in the short-term memory.

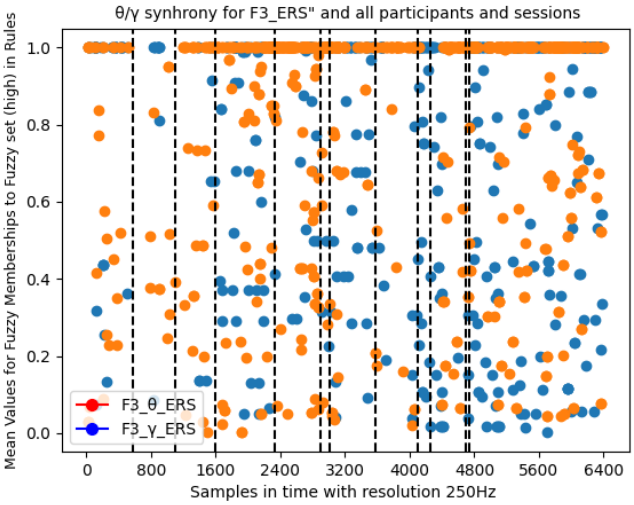

Fig. 10. θ/γ synchrony for F3_ERS″ averaged across all participants

VI. RESULTS AND DISCUSSION

By experiments we proved that visual node-based programming framework for BCI applications utilizing pre-existing nodes within Node-RED to register and analyze EEG signals from OpenBCI headsets, for the purpose of sending control commands to a robotic arm, streamlines the design process and minimizes the need for extensive programming. At the same time, after analyzing the EEG data and gathering knowledge from the experiment, we made conclusions about neuronal activity related to mental intentions for controlling smart home devices.

Indeed, in line with our hypothesis, we anticipated that following the experiments, we might identify a universal threshold for the BrainFlow performance metric. After averaging the values for the mindfulness metric (MV), calculated using the BrainFlow software and extended with data from 7 additional participants, we observed a consistent threshold of approximately 0.31 with a standard deviation of 0.11. Although this value is slightly higher than that reported in [19], it still indicates consistency in the results, as the re-evaluated MV threshold shows moderate inter relative variability (CV ≈ 0.364). We attribute this to younger age of the new participants (21 years) and the baseline calibration. MV depends on various factors, such as baseline attention, external distractions, mental fatigue and others. When calculating intra-variability, most participants showed low to moderate intra-variability (0.04–0.07), with minimal concentration fluctuation and better focus. Such low variability suggests that their overall performance was fairly consistent. However, some participants displayed higher variability, with scores between 0.1 and 0.2. This indicates less consistency in maintaining focus, due to various factors mentioned earlier. Three participants were asked to repeat the experiment. Two reported that the white screen used during the baseline phase was irritating, so we replaced it with a light grey background. One participant wore a smartwatch, which interfered with and compromised the results.

We did not measure system's latency because the delay observed during the trial is in milliseconds and is imperceptible to the participant, meaning it does not affect the real-time experience of controlling the robotic arm. Additionally, the time

required for each participant to reach the necessary concentration level varies, as individual cognitive processes differ. For performance evaluation, we focused on the BCI's ability to recognize user intent, as system latency had no noticeable impact on interaction.

In line with our hypothesis, we detected bursts in β_2 and γ ERS over the prefrontal, parietal and near primary motor cortex (Cz) that would correlate with attention and concentration. Compared to the previous results in [19], some of the middle bars in Fig. 9 have shifted positions, indicating a slight change in the ranking of electrodes and frequency bands based on their mean ERS″ values during high MV. Since the overall pattern remains consistent, these shifts are negligible. Although the higher standard deviation of MV is likely influenced by baseline calibration or age, the second derivative of ERS in EEG frequency powers is relative and slightly affected by baseline calibration, making it a reliable neuromarker to distinguish normal fluctuations from significant events.

Although the β_2 ERS″ is not dominant, our findings are consistent with the research reported in [31] and [32], which indicate such correlation with attentiveness. We observed considerable θ activity, consistent with references [29] and [30]. The predominant θ and γ bursts in ERS (Fig. 9) during solving of math problems on one hand, require memorizing intermediate calculations (θ) and, on the other hand, require high concentration (γ) during the addition, subtraction, multiplication, and division of floating-point numbers. This observation aligns with [26] and [27], where it is noted that low-frequency oscillations (5 to 12 Hz), such as θ waves, establish a temporal framework for organizing brain activity and memory processing. Within this framework, high-frequency subcycles (40 Hz), or γ waves, facilitate the rapid encoding and retrieval of information, enabling the brain to efficiently manage and retain multiple pieces of information simultaneously. These patterns coexist within a single neural network by fitting distinct γ subcycles into a θ oscillation, reflecting the rhythmic patterns of neuronal firing and temporal nesting. This phenomenon is also evident in our findings specifically for θ/γ synchrony for F3_ERS″ (see Fig. 10). The results in this figure slightly differ from those presented in [19] and replicate these rhythmic patterns.

VII. Conclusion

Through experiments, we successfully validated the proposed visual node-based programming framework for BCI applications utilizing the openBCI toolkit within Node-RED for integrating OpenBCI Cyton+Daisy Boards with the TinkerKit Braccio robotic arm for smart home control. We identified key electrodes and frequency bands linked to attention and concentration for robotic arm control, as well as the average threshold for the 'Mindfulness' metric proposed by the BrainFlow library. In the future, we plan to integrate BCIs with Explainable AI (XAI) to enable transparent home automation with clearly explaining why devices like lights, thermostats, entertainment systems respond to mental states such as intention, focus or relaxation.

References

[1] M. K. Islam and A. Rastegarnia, "Editorial: Recent advances in EEG (non-invasive) based BCI applications," Frontiers in Computational Neuroscience, vol. 17, 2023, Art. no. 1151852, doi: 10.3389/fncom.2023.1151852.

[2] B. Maiseli, A. T. Abdalla, L. V. Massawe, et al., "Brain–computer interface: trend, challenges, and threats," Brain Informatics, vol. 10, p. 20, 2023, doi: 10.1186/s40708-023-00199-3.

[3] M. Al-Mohammadi, A. Al-Nuaimi and L. B. Farah, "Smart home based on BCI for disabled people: A state-of-the-art review," in AIP Conf. Proc., vol. 3232, no. 1, 2024, AIP Publishing.

[4] V. Santhi, Y. N. V. S. Sabareesh, P. P. Sudheer and V. P. Sai Krishna, "Trends and challenges in AIoT implementation for smart homes, smart buildings, and smart cities in cloud platforms," in Artificial Intelligence of Things (AIoT) for Productivity and Organizational Transition, pp. 240–319, 2024.

[5] A. Zakzouk, K. Menzel and M. Hamdy, "Brain-Computer-Interface (BCI) Based Smart Home Control Using EEG Mental Commands," in Collaborative Networks in Digitalization and Society 5.0 (PRO-VE 2023), IFIP AICT, vol. 688, Springer, Cham, 2023.

[6] B. B. Borah, U. Hazarika, S. M. B. Baruah, S. Roy and A. Jamir, "A BCI framework for smart home automation using EEG signal," Intelligent Decision Technologies, vol. 17, no. 2, pp. 485–503, 2023, doi: 10.3233/IDT-220224.

[7] M.-V. Drăgoi, I. Nisipeanu, A. Frimu, A.-M. Tălîngă, A. Hadăr, T. G. Dobrescu, C. P. Suciu and A. R. Manea, "Real-Time Home Automation System Using BCI Technology," Biomimetics, vol. 9, no. 10, p. 594, 2024, doi: 10.3390/biomimetics9100594.

[8] S. Cariello, D. Sanalitro, A. Micali, A. Buscarino and M. Bucolo, "Brain–Computer-Interface-Based Smart-Home Interface by Leveraging Motor Imagery Signals," Inventions, vol. 8, no. 4, p. 91, 2023, doi: 10.3390/inventions8040091.

[9] O. A. Rușanu, "The Development of Brain-Computer Interface Applications Controlled by the Emotiv Insight Portable Headset Based on Analyzing the EEG Signals Using NODE-Red and Python Programming Software Tools," in Open Science in Engineering (REV 2023), Lecture Notes in Networks and Systems, vol. 763, Springer, Cham, 2023.

[10] B. Wutzl, K. Leibnitz and M. Murata, "An analysis of the correlation between the asymmetry of different EEG-sensor locations in diverse frequency bands and short-term subjective well-being changes," Brain Sciences, vol. 14, no. 3, p. 267, 2024.

[11] S. G. Mason and G. E. Birch, "A general framework for brain-computer interface design," IEEE Trans. Neural Syst. Rehabil. Eng., vol. 11, no. 1, pp. 70–85, Mar. 2003, doi: 10.1109/TNSRE.2003.810426.

[12] Neuroscale, [Online]. Available: https://neuroscale.intheon.io/. [Accessed: Jan. 2024].

[13] EmotivBCI Node-RED toolkit, [Online]. Available: https://emotiv.gitbook.io/emotivbci-node-red-toolbox/. [Accessed: Jan. 2024].

[14] openBCI toolkit within the Node-RED platform, [Online]. Available: https://flows.nodered.org/collection/W7dKrufq2WWR. [Accessed: Jan. 2024].

[15] MetaBCI: An Open-Source Platform for Brain-Computer Interfaces, [Online]. Available: https://doi.org/10.1016/j.compbiomed.2023.107806. [Accessed: Jan. 2024].

[16] Y. Renard, F. Lotte, G. Gibert, M. Congedo, E. Maby, V. Delannoy, O. Bertrand and A. Lécuyer, "OpenViBE: An Open-Source Software Platform to Design, Test and Use Brain-Computer Interfaces in Real and Virtual Environments," Presence, vol. 19, no. 1, pp. 35–53, 2010, doi: 10.1162/pres.19.1.35.

[17] Node-RED, [Online]. Available: https://nodered.org/. [Accessed: Jan. 2024].

[18] BrainFlow software library, [Online]. Available: https://github.com/brainflow-dev/brainflow. [Accessed: Jan. 2025].

[19] A. Kremenska, A. Lekova and G. Dimitrov, "Validating the OpenBCI Nodes within the Node-RED Library through an EEG-based BCI Application for IoT," in Proc. 2024 Int. Conf. on Software, Telecommunications and Computer Networks (SoftCOM), Split, Croatia, 2024, pp. 1–6, doi: 10.23919/SoftCOM62040.2024.10721977.

[20] TinkerKit Braccio robot arm, [Online]. Available: https://store.arduino.cc/products/tinkerkit-braccio-robot. [Accessed: Jan. 2025].
[21] OpenBCI, [Online]. Available: https://openbci.com/. [Accessed: Jan. 2024].
[22] OpenBCI Citation List, [Online]. Available: https://docs.openbci.com/citations/. [Accessed: Jan. 2025].
[23] BrainFlow user APIs, [Online]. Available: https://brainflow.readthedocs.io/en/stable/UserAPI.html. [Accessed: Jan. 2025].
[24] A. Kremenska and A. Lekova, "New Nodes for Node-RED Library within OpenBCI Category for EEG-Based Brain-Machine Interface Design and Integration in IoT," Preprints, 2024, Art. no. 2024011608, doi: 10.20944/preprints202401.1608.v1.
[25] D. Osipova, A. Takashima, R. Oostenveld, G. Fernández, E. Maris and O. Jensen, "Theta and gamma oscillations predict encoding and retrieval of declarative memory," J. Neurosci., vol. 26, no. 28, pp. 7523–7531, 2006.
[26] J. E. Lisman and M. A. Idiart, "Storage of 7±2 short-term memories in oscillatory subcycles," Science, vol. 267, no. 5203, pp. 1512–1515, 1995.
[27] G. Soroka, M. Idiart and A. Villavicencio, "Mechanistic role of alpha oscillations in a computational model of working memory," PLOS One, vol. 19, no. 2, Art. no. e0296217, 2024.
[28] T. Sigurdsson and S. Duvarci, "Hippocampal-prefrontal interactions in cognition, behavior and psychiatric disease," Front. Syst. Neurosci., vol. 9, p. 190, 2016.
[29] A. R. Clarke, R. J. Barry, D. Karamacoska and S. J. Johnstone, "The EEG Theta/Beta Ratio: A marker of Arousal or Cognitive Processing Capacity?" Appl. Psychophysiol. Biofeedback, vol. 44, no. 2, pp. 123–129, 2019, doi: 10.1007/s10484-018-09428-6.
[30] C. Picken, A. R. Clarke, R. J. Barry, R. McCarthy and M. Selikowitz, "The Theta/Beta Ratio as an Index of Cognitive Processing in Adults with the Combined Type of Attention Deficit Hyperactivity Disorder," Clin. EEG Neurosci., vol. 51, no. 3, pp. 167–173, 2020, doi: 10.1177/1550059419895142.
[31] H. Heinrich, K. Busch, P. Studer, K. Erbe, G. H. Moll and O. Kratz, "EEG spectral analysis of attention in ADHD: implications for neurofeedback training," Front. Hum. Neurosci., vol. 8, p. 611, 2014.
[32] N. H. Liu, C. Y. Chiang and H. C. Chu, "Recognizing the degree of human attention using EEG signals from mobile sensors," Sensors, vol. 13, no. 8, pp. 10273–10286, 2013, doi: 10.3390/s130810273.
[33] A. Lekova and I. Chavdarov, "A Fuzzy Shell for Developing an Interpretable BCI Based on the Spatiotemporal Dynamics of the Evoked Oscillations," Comput. Intell. Neurosci., vol. 2021, Art. ID 6685672, 21 pages, 2021, doi: 10.1155/2021/6685672.

Adelina Kremenska holds an M.Sc. degree in Telecommunications from the Technical University of Sofia and a Ph.D. in Electrical Engineering, Electronics, and Automation from the Bulgarian Academy of Sciences (BAS). She is currently an engineer at the Institute of Robotics, BAS, where her research focuses on EEG-based Brain-Computer Interfaces and Socially Assistive Robotics (SARs).

Anna Lekova has received M.Sc. and Ph.D. degrees in Computer Science from the Technical University, Sofia. She is currently a Professor in the Institute of Robotics and a Head of "Interactive Robotics and Control Systems" Department. Her current research interests are in Socially-assistive Robotics (SARs) and EEG-based Brain-Computer Interfaces. Current projects, publications and citations can be seen https://orcid.org/0000-0002-9012-4714 .

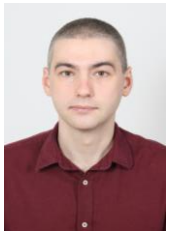

Svetoslav Kremenski holds an M.Sc. degree in Telecommunications from the Technical University, Sofia. Currently, he is a Ph.D. student at the Institute of Robotics, Bulgarian Academy of Sciences.

Georgi Petrov Dimitrov is a Professor in the University of Library Studies and Information Technologies, Sofia, Bulgaria. Dean of the Faculty of Information Systems and Technologies. His current research interests are Brain Computer Interface, Artificial Intelligence, Robotics and IoT. https://orcid.org/0000-0002-4785-0702